Ultrafast Photoinduced Electron Transfer in Rigid Porphyrin-Quinone Dyads

Alisdair N. Macpherson, Paul A. Liddell, Su Lin, Lori Noss, Gilbert R. Seely, Janice M. DeGraziano, Ana L. Moore,* Thomas A. Moore,* and Devens Gust*

Contribution from the Center for the Study of Early Events in Photosynthesis, Department of Chemistry and Biochemistry, Arizona State University, Tempe, Arizona 85287-1604

Received January 11, 1995[⊗]

Abstract: Three dyad molecules, each consisting of a porphyrin (P) linked to a quinone (Q) through a rigid bicyclic bridge, have been prepared, and their photochemistry has been investigated using time-resolved fluorescence and absorption techniques. In all three molecules, photoinduced electron transfer from the porphyrin first excited singlet state to the quinone occurs with rate constants of $\sim 10^{12}$ s^{-1} in solvents ranging in dielectric constant from ~2.0 to 25.6 and at temperatures from 77 to 295 K. The transfer rate is also relatively insensitive to thermodynamic driving force changes up to 0.4 eV. This behavior is phenomenologically similar to photosynthetic electron transfer. The rapid rate of photoinduced electron transfer and its lack of dependence on environmental factors suggests that transfer is governed by intramolecular vibrations. Charge recombination of $P^{\bullet+}-Q^{\bullet-}$, on the other hand, is substantially slower than charge separation and sensitive to both driving force and environmental conditions. Thus, by changing conditions, charge recombination rates can be varied over a wide range while photoinduced electron transfer rates are relatively unaffected. This suggests that rigid dyads of this general type may be useful building blocks for more complex molecular devices.

Introduction

Some of the most intriguing aspects of photoinduced electron transfer in photosynthetic reaction centers are the rapidity of the process in the relatively rigid protein matrix and its apparent insensitivity to temperature and thermodynamic driving force.[1-5] In contrast, the majority of photosynthetic model systems display photoinduced electron transfer rates that are strong functions of driving force and environmental factors. Most also have molecular structures in which the donor-acceptor electronic interactions are subject to modification by internal rotations.

Covalently linked porphyrin-quinone dyads constitute one of the most thoroughly investigated classes of photosynthetic models.[1,6-10] Essentially all of these molecules include at least one single bond in the linkage between the two moieties. Rotation about such bonds can modulate the electronic interactions between the porphyrin electron donor and the quinone acceptor and thus affect the electron transfer rates, which depend strongly upon such interactions. The presence of single bonds usually introduces ambiguities concerning the most stable molecular conformation, the nature of any transient conformations from which electron transfer may occur, and the effects of intramolecular motions upon observed electron transfer rates.

In some cases, the effects of such motions have been reduced by rigidly linking a quinone acceptor to an aryl group that is attached by a single bond to a *meso*-position on the porphyrin macrocycle. Such aryl groups oscillate about this bond, and the rotation modulates internuclear separations and orientations and therefore the electronic coupling between the ring and the macrocycle. This rotation may be limited by placing substituents at the pyrrole β-positions flanking the aryl ring.[6,9] The resulting steric hindrance reduces rotational motions about the single bond but may not completely eliminate them.

In one case,[11] clever synthetic methodology has been developed for linking a porphyrin moiety to a quinone through a quinoxalino group, which achieves a well-defined, rigid structure. A consequence of this particular strategy is that the porphyrin π-electron system is modified and extended by conjugation with the quinoxalino bridge. The observed electron transfer rates are slow relative to those in photosynthetic reaction centers and depend significantly on solvent polarity.

Most porphyrin-quinone model systems exhibit photoinduced electron transfer rates that depend upon temperature and the reaction medium.[6,8,9] In fact, electron transfer is usually not observable at low temperatures, whereas in reaction centers, the process occurs at liquid helium temperatures. Recently, electron transfer in low-temperature glasses has been achieved in model systems that are designed to have a large thermodynamic driving force for electron transfer at room temperature in polar media, and this has allowed the exploration of a variety of magnetic phenomena which have previously been unobservable.[9,12] As mentioned above, however, photosynthetic photoinduced electron transfer rates evidently depend only weakly on both driving force and temperature.

⊗ Abstract published in *Advance ACS Abstracts*, June 1, 1995.

(1) Bixon, M.; Fajer, J.; Feher, G.; Freed, J. H.; Gamliel, D.; Hoff, A. J.; Levanon, H.; Mobius, K.; Nechushtai, R.; Norris, J. R.; Scherz, A.; Sessler, J. L.; Stehlik, D. *Isr. J. Chem.* **1992**, *32*, 449-455.

(2) Norris, J. R.; Schiffer, M. *Chem. Eng. News* **1990**, *68*, 22-37.

(3) Feher, G.; Allen, J. P.; Okamura, M. Y.; Rees, D. C. *Nature (London)* **1989**, *339*, 111-116.

(4) Woodbury, N. W.; Peloquin, J. M.; Alden, R. G.; Lin, X.; Lin, S.; Taguchi, A. K. W.; Williams, J. C.; Allen, J. P. *Biochemistry* **1994**, *33*, 8101-8112.

(5) Peloquin, J. M.; Williams, J. C.; Lin, X.; Alden, R. G.; Taguchi, A. K. W.; Allen, J. P.; Woodbury, N. W. *Biochemistry* **1994**, *33*, 8089-8100.

(6) Connolly, J. S.; Bolton, J. R. In *Photoinduced electron transfer*; Fox, M. A., Channon, M., Eds.; Elsevier: Amsterdam, 1988; Part D, pp 303-393.

(7) Gust, D.; Moore, T. A. *Adv. Photochem.* **1991**, *16*, 1-65.

(8) Gust, D.; Moore, T. A.; Moore, A. L. *Acc. Chem. Res.* **1993**, *26*, 198-205.

(9) Wasielewski, M. R. *Chem. Rev.* **1992**, *92*, 435-461.

(10) Asahi, T.; Ohkohchi, M.; Matsusaka, R.; Mataga, N.; Zhang, R. P.; Osuka, A.; Maruyama, K. *J. Am. Chem. Soc.* **1993**, *115*, 5665-5674.

(11) Antolovich, M.; Keyte, P. J.; Oliver, A. M.; Paddon-Row, M. N.; Kroon, J.; Verhoeven, J. W.; Jonker, S. A.; Warman, J. M. *J. Phys. Chem.* **1991**, *95*, 1933-1941.

0002-7863/95/1517-7202$09.00/0

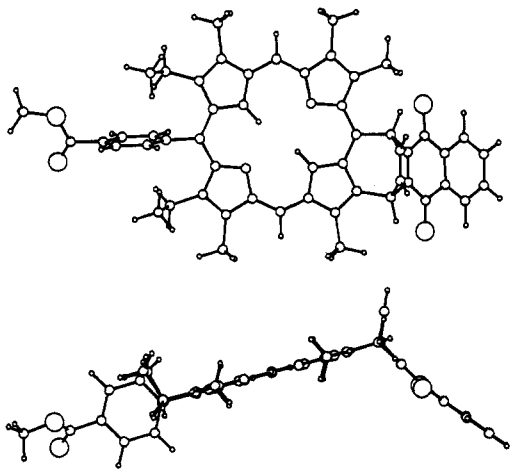

Figure 1. Solution conformation of porphyrin–quinone dyad **1** as calculated using molecular mechanics methods.

In order to explore these effects more thoroughly, we have designed a new class of porphyrin–quinone dyads that feature both rigid, nonconjugated hydrocarbon bridges between the donor and acceptor and relatively strong electronic coupling between these moieties and, therefore, might be expected to display enhanced electron transfer rates in viscous, nonpolar media and at low temperatures. Herein we report the synthesis and spectroscopic study of the first of these molecules, dyads **1–3**, in which the porphyrin electron donor and quinone acceptor are joined by short bicyclic bridges.

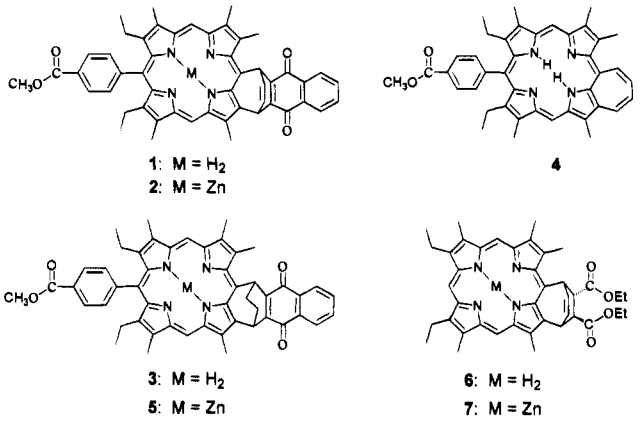

Results

Synthesis. Dyad **1** was synthesized by the Diels–Alder reaction using a new class of porphyrin diene whose preparation we recently described.[13] Heating a solution of diene **4** and naphthoquinone at 176 °C in 1,2-dichlorobenzene gave **1** in 72% yield. Zinc was inserted quantitatively by treating a dichloromethane solution of **1** with methanolic zinc acetate. Reduction of the resulting dyad **2** gave **5**, and removal of the zinc with trifluoroacetic acid produced **3**. Compounds **1–4** were characterized by mass spectrometry and 500 MHz ^{1}H NMR spectroscopy (COSY, NOESY, HMBC, HMQC) (see the Experimental Section).

Molecular Conformation. The conformation of dyad **1** shown in Figure 1 is derived from molecular mechanics calculations performed using the CHARMm program in the QUANTA molecular modeling package from Polygen Corp. The calculations involved defining the force fields for the various components followed by energy minimization. The force fields were assigned by the choice of suitable atom-type parameters that combine to define the force constants for the various bonds and other interactions. For most of the atoms, the usual CHARMm atom types were retained. However, it was necessary to increase the constants for torsion about the bonds in the porphyrin macrocycle in order to allow the program to minimize a normal porphyrin to a relatively planar structure similar to those observed by X-ray crystallography. The minimization procedure was an adopted-basis Newton–Raphson method suitable for relatively large molecules. The dihedral angle between the planes of the porphyrin and the quinone is ~120°, and the center-to-center separation of the two chromophores is 6.7 Å.

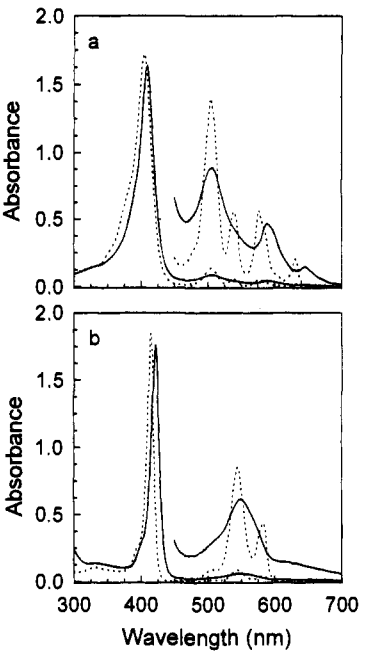

Figure 2. (a) Absorption spectra of dyad **1** (—) and model porphyrin **6** (- - -) in 2-methyltetrahydrofuran solution at ambient temperature. The inset is a 10-fold expansion of the Q-band region. (b) Absorption spectra of zinc dyad **2** (—) and model porphyrin **7** (- - -) in 2-methyltetrahydrofuran solution at ambient temperature. The inset is a 10-fold expansion of the Q-band region.

Electrochemistry. Cyclic voltammetric studies of **1** in benzonitrile yielded a first oxidation potential for the porphyrin of 0.422 V and a first reduction potential for the quinone of −1.148 V vs a ferrocene internal reference redox system. Similar experiments with **2** gave first oxidation and reduction potentials of 0.211 and −1.180 V, respectively. The first oxidation potentials for model porphyrins **6** and **7** are 0.359 and 0.177 V.

Steady-State Absorption Spectra. Figure 2a shows the absorption spectra of **1** and model porphyrin[13] **6** in 2-methyltetrahydrofuran. Porphyrin **6** displays the Soret maximum at 405 nm and Q-bands at 504, 538, 576, and 631 nm. The Soret band of **1** is shifted slightly to 409 nm. The Q-bands are substantially broadened, and maxima are observed at 507, 589, and 646 nm. Dyad **3**, in which the double bond of the bicyclic bridge has been reduced, has an absorption spectrum whose shape is similar to that of **1**, but the maxima (406, 505, 583, and 636 nm) are less shifted relative to **6**. Similar effects were noted for the zinc dyad **2** (Figure 2b). Model porphyrin **7** has bands at 415 (Soret), 545, and 583 nm. In **2**, the Soret band

(12) Wasielewski, M. R.; Gaines, G. L., III; O'Neil, M. P.; Svec, W. A.; Niemczyk, M. P.; Prodi, L.; Gosztola, D. In *Dynamics and Mechanisms of Photoinduced Transfer and Related Phenomena*; Mataga, N., Okada, T., Masuhara, H., Eds.; Elsevier Science Publishers: New York, 1992; pp 87–103.

(13) Liddell, P. A.; Demanche, L. J.; Li, S.; Macpherson, A. N.; Nieman, R. A.; Moore, A. L.; Moore, T. A.; Gust, D. *Tetrahedron Lett.* **1994**, *35*, 995–998.

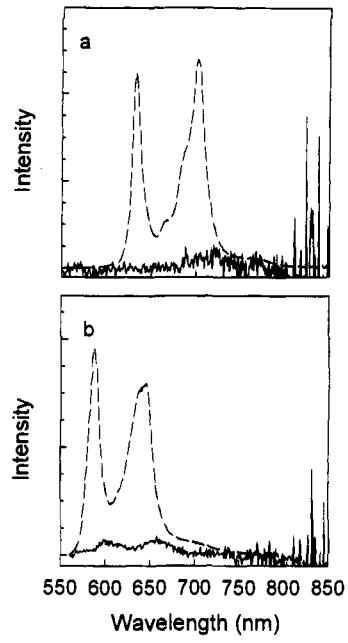

Figure 3. (a) Emission spectra of model porphyrin **6** (− −) and dyad **1** (—) in 2-methyltetrahydrofuran solution at ambient temperature. The solutions had the same absorbance at the excitation wavelength (500 nm). The emission intensity from the dyad has been multiplied by a factor of 100. (b) Emission spectra of model porphyrin **7** (− −) and dyad **2** (—) in 2-methyltetrahydrofuran solution at ambient temperature. The solutions had the same absorbance at the excitation wavelength (550 nm). The emission intensity from the dyad has been multiplied by a factor of 10. The very low intensity emissions from the dyad samples likely result from trace porphyrin impurities.

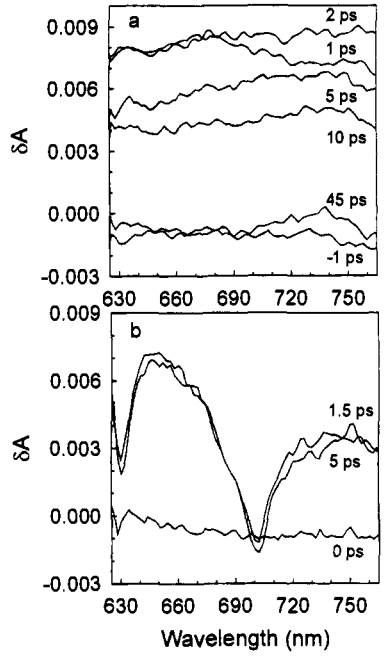

Figure 4. (a) Long-wavelength region transient absorption spectra obtained after excitation of a solution of dyad **1** in 2-methyltetrahydrofuran at 295 K with a 590-nm, ~200-fs laser pulse. The spectra were measured using the pump—probe technique and are corrected for dispersion. The featureless transient absorption is characteristic of the porphyrin radical cation in the $P^{\bullet+}$—$Q^{\bullet-}$ charge-separated state. (b) Spectra from similar transient absorption experiments with model porphyrin **6**. The minima represent stimulated emission from the porphyrin first excited singlet state, which does not decay on the time scale of the measurement.

appears at 422 nm and the Q-band region consists of a broad absorption at 548 nm with a broad shoulder at ~625 nm.

Steady-State Fluorescence Spectra. The fluorescence emission spectrum of porphyrin **6** (Figure 3a) features maxima at 633 and 702 nm in 2-methyltetrahydrofuran, and the emission quantum yield is 0.067 (measured by the comparative method with tetraphenylporphyrin as a standard[14]). Zinc porphyrin **7** emits with maxima at 587 and 645 nm and a quantum yield of 0.034 (Figure 3b). No steady-state fluorescence emission uniquely attributable to any of the porphyrin—quinone dyads could be observed. The quantum yields are $\leq 3 \times 10^{-5}$, $\leq 5 \times 10^{-4}$, and $\leq 1 \times 10^{-4}$ for **1**, **2**, and **3**, respectively. These values are only upper limits because tiny amounts of fluorescent impurities, such as dyad containing reduced quinone, will contribute substantially to the steady-state measurements. The strong quenching of the porphyrin first excited singlet states is ascribed to photoinduced electron transfer to yield the $P^{\bullet+}$—$Q^{\bullet-}$ charge-separated states as has been observed in many other porphyrin—quinone systems.[1,6-10]

Time-Resolved Fluorescence Studies. A solution of model porphyrin **6** in 2-methyltetrahydrofuran was excited with laser pulses at 590 nm, and its fluorescence decay was measured by the time-correlated single photon counting method. The fluorescence, monitored at 702 nm, decayed as a single exponential with a lifetime of 11.3 ns ($\chi^2 = 1.17$). Excitation of a similar solution of dyad **1** at 620 nm and detection of the fluorescence at 730 nm (a region with little Raman scattering) yielded a decay consisting mainly (99.6%) of a single-exponential component with a lifetime of 0.9 ps ($\chi^2 = 1.01$). Measurements at other wavelengths also gave lifetimes of ~1 ps. The instrument response function was 35 ps. Reconvolution analysis of well-behaved sets of fluorescence data can yield reliable decay lifetimes down to ~5 ps; lifetimes shorter than this are of questionable validity. Thus, the 1 ps lifetime is only an approximate upper limit to the actual fluorescence lifetime. The results are compatible with the steady-state results mentioned above, which yield a lifetime for the porphyrin first excited singlet state of **1** of ≤5 ps, based on the lifetime and fluorescence quantum yield of model porphyrin **6**. Excitation of a 2-methyltetrahydrofuran solution of **3** with 590-nm laser pulses and detection at 655 nm produced a decay that was analyzed in terms of two exponential components ($\chi^2 = 1.16$) of 2.0 ps (99.2% of the initial amplitude) and 11 ns (0.8% of the initial amplitude).

Excitation of zinc porphyrin **7** in 2-methyltetrahydrofuran with a 570-nm laser pulse followed by detection of the fluorescence at 590 nm gave a single-exponential decay with a time constant of 2.01 ns ($\chi^2 = 1.11$). Excitation of a similar solution of zinc-containing dyad **2** at 570 nm and detection at 660 nm yielded a major (97.6%) decay component with a lifetime of 2.3 ps ($\chi^2 = 1.07$). This upper limit for the lifetime of the porphyrin first excited singlet state is compatible with the steady-state results.

Time-Resolved Absorption Spectra. In order to further investigate the strong fluorescence quenching noted above, greater time resolution was necessary, and time-resolved absorption measurements on the sub-picosecond time scale were undertaken. Excitation of a $\sim 5 \times 10^{-4}$ M solution of model porphyrin **6** in 2-methyltetrahydrofuran with 150—200 fs, 590-nm laser pulses led to the appearance of the transient spectra shown in Figure 4b. The main features are the two stimulated emission bands corresponding to porphyrin fluorescence (see Figure 3a). The spectrum rises with a time constant of 0.26

(14) Gust, D.; Moore, T. A.; Moore, A. L.; Macpherson, A. N.; Lopez, A.; DeGraziano, J. M.; Gouni, I.; Bittersmann, E.; Seely, G. R.; Gao, F.; Nieman, R. A.; Ma, X. C.; Demanche, L. J.; Hung, S.-C.; Luttrull, D. K.; Lee, S.-J.; Kerrigan, P. K. *J. Am. Chem. Soc.* **1993**, *115*, 11141—11152.

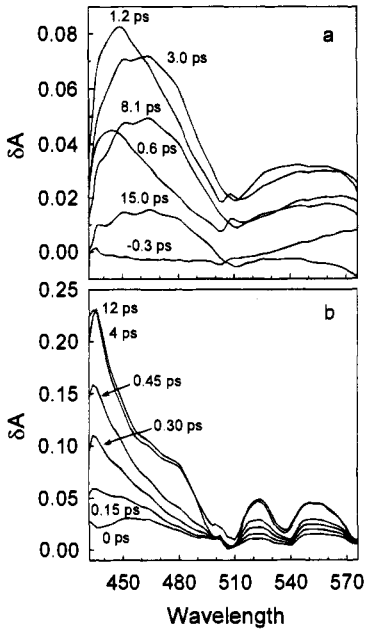

Figure 5. (a) Short-wavelength region transient absorption spectra obtained after excitation of a solution of dyad **1** in 2-methyltetrahydrofuran at 295 K with a 590-nm, ~200-fs laser pulse. The spectra were measured using the pump–probe technique and are corrected for dispersion. The broad absorption is consistent with ultrafast formation of the porphyrin radical cation by electron transfer. The minimum at ~507 nm corresponds to a ground-state absorption maximum. (b) Transient spectra for model porphyrin **6** obtained under similar conditions. The minima correspond to ground-state absorption bands.

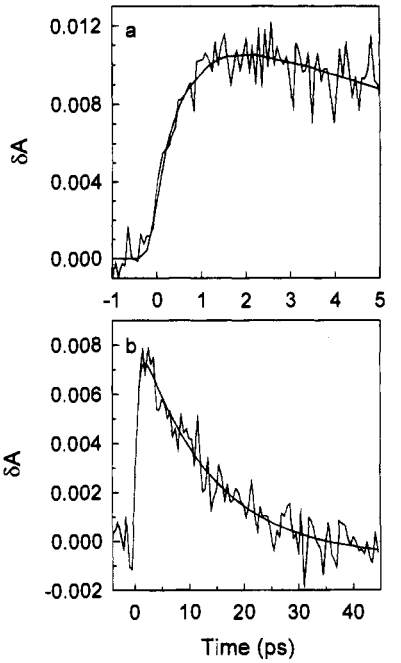

Figure 6. Rise (a) and decay (b) of the transient absorption spectrum of **1** shown in Figure 5a, as determined in the 630–640-nm region. The formation consists of a prompt component (presumably due to ^{1}P–Q) followed by a slower rise of $P^{\bullet+}$–$Q^{\bullet-}$ with a time constant of 0.70 ps, as determined by deconvolution from the excitation pulse. The decay lifetime of $P^{\bullet+}$–$Q^{\bullet-}$ is 13 ps.

ps, as measured in the 630–640 nm region, which is close to the excitation pulse width. The transient absorption does not decay appreciably on the time scale of several hundred picoseconds and is assigned to the porphyrin first excited singlet state. Figure 4a shows the spectra resulting from excitation of a 2-methyltetrahydrofuran solution of dyad **1**. The featureless transient absorption lacking any sign of stimulated emission in the spectral region where porphyrin fluorescence is expected is consistent with assignment to the porphyrin radical cation, rather than the porphyrin first excited singlet state. Thus, the results suggest rapid formation and subsequent decay of the $P^{\bullet+}$–$Q^{\bullet-}$ charge-separated state, as discussed above.

The transient spectra in the shorter-wavelength region are shown in Figure 5. The spectra of model porphyrin **6** (Figure 5b) display minima at ~505, 538, and 575 nm, which correspond to Q-band maxima in the ground-state absorption spectrum, superimposed upon the broad transient absorption of the first excited singlet state. The spectrum does not decay on the picosecond time scale. Dyad **1** (Figure 5a) shows the rapid appearance of a broad absorption with a maximum in the 460-nm region upon which is superimposed a minimum corresponding to the ground-state absorption band at 507 nm. The transient signal decays over a period of several picoseconds and is consistent with assignment to $P^{\bullet+}$–$Q^{\bullet-}$.

The time dependence of the transient absorption of **1** in the 630–640 nm region is shown in Figure 6. Figure 6a shows the rise of the signal, which consists of a prompt absorption that appears with the excitation pulse (presumably ^{1}P) followed by a slower increase with a time constant of 0.70 ps. This second rise time is significantly slower than the 0.26 ps rise of ^{1}P in model porphyrin **6** and is attributed to the formation of $P^{\bullet+}$–$Q^{\bullet-}$ from ^{1}P–Q. The time constant for decay of $P^{\bullet+}$–$Q^{\bullet-}$ is 13 ps (Figure 6b).

Excitation of zinc porphyrin **7** in 2-methyltetrahydrofuran solution at 590 nm is followed by the appearance of a transient spectrum in the 630–780 nm region which displays stimulated emission at 645 nm, corresponding to the longest-wavelength fluorescence band of this molecule. The transient rises with a time constant of ~0.17 ps (the width of the excitation pulse) and does not decay appreciably on the tens-of-picoseconds time scale. Excitation of zinc dyad **2** under similar conditions results in the appearance of a transient absorption similar to that in Figure 4a, but displaying a broad maximum at ~700 nm (see also Figure 7b). Stimulated emission is not observed. The transient absorption rises with a time constant of ~0.23 ps and decays in 5.2 ps. These results are fully consistent with the steady-state and time-resolved fluorescence data and are attributed to the rapid formation of a $P_{Zn}^{\bullet+}$–$Q^{\bullet-}$ charge-separated state. The zinc porphyrin radical cation is known to display a broad absorption maximum in the 700-nm region.[12]

Effect of Temperature. Solutions of **1**, **2**, or **3** in 2-methyltetrahydrofuran form a clear glass at 77 K. The absorption spectra of these glasses show band shapes similar to those observed at ambient temperatures, but the maxima are blue shifted by 1–7 nm. Excitation of such a glass containing dyad **1** with 590-nm laser pulses leads to the transient absorption spectra shown in Figure 7a. A broad absorption appears immediately after excitation and decays over several hundred picoseconds. The spectrum displays a small negative feature at 630 nm, corresponding to bleaching of the longest-wavelength absorption band of **1**, but no stimulated emission from a porphyrin excited singlet state. Thus, as with the room-temperature spectra, these low-temperature results are consistent with the rapid formation and slower decay of $P^{\bullet+}$–$Q^{\bullet-}$.

Excitation of a glass containing zinc dyad **2** at 77 K under similar conditions led to the observation of the transient spectrum shown in Figure 7b. A broad absorption with a maximum at about 700 nm, characteristic of the zinc porphyrin radical cation, appears immediately after excitation. Stimulated emission characteristic of a zinc porphyrin excited state is not observed.

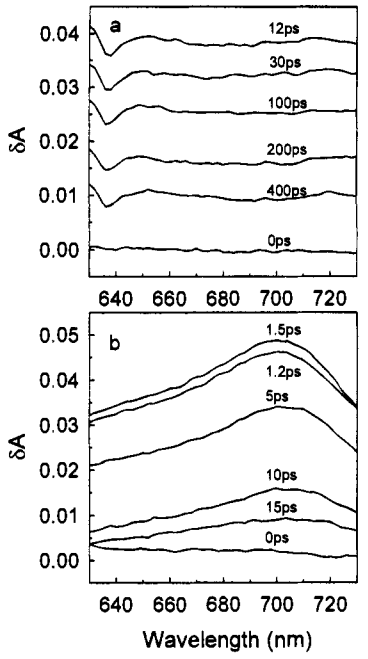

Figure 7. Time-resolved transient absorption spectra at 77 K obtained after excitation of dyads **1** (a) and **2** (b) in a 2-methyltetrahydrofuran glass with ~200-fs, 590-nm laser pulses. The spectra, which are corrected for dispersion effects, are characteristic of the porphyrin radical cations of the charge-separated species. In the case of the metalated porphyrin of **2**, the radical cation spectrum features a broad maximum at ~700 nm.

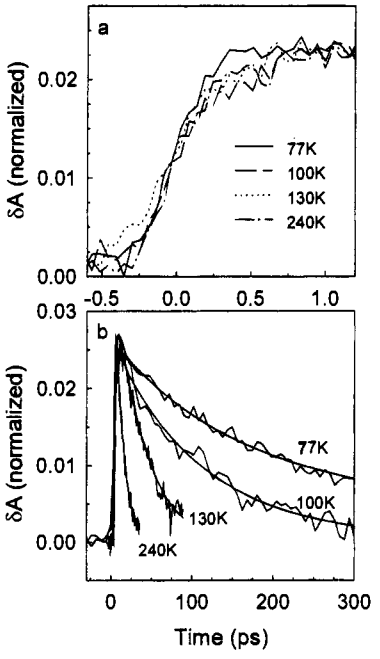

Figure 8. Rise (a) and decay (b) of the transient absorption in the 670-nm region for dyad **1**, obtained at various temperatures in 2-methyltetrahydrofuran following excitation as described for Figure 6. The rise times are all on the order of 0.7 ps. The decay times for the transients in b vary with temperature. The best single-exponential fits to the decay data are shown and lead to the lifetimes reported in the text.

The rise of the transient absorption of dyad **1** in the 670-nm region following excitation at 590 nm is shown as a function of temperature in Figure 8a. The rise time of $P^{\bullet+}-Q^{\bullet-}$ is ~0.7 ps down to 100 K, and perhaps slightly shorter at 77 K, although the signal-to-noise ratio renders this last conclusion somewhat speculative. The decay of the transient as a function of temperature is shown in Figure 8b. The lifetimes, analyzed as single exponentials, are 10, 38, 112, and 148 ps at 240, 130, 100, and 77 K, respectively. The calculated decays with these time constants are also shown in Figure 8b. At 77 K in the 2-methyltetrahydrofuran glass, the transient absorption assigned to $P_{Zn}^{\bullet+}-Q^{\bullet-}$ (Figure 7b) rises with a time constant of ~0.33 ps and decays with a lifetime of 6.6 ps. In all of these cases, the rise time is associated with formation of the charge-separated state and the decay with its recombination.

Low-temperature steady-state fluorescence emission results are consistent with this interpretation. The emission spectrum of model porphyrin **6** in the glass at 77 K has maxima at 626 and 694 nm. Time-resolved studies yield an excited singlet state lifetime of 14.8 ns. If one assumes that the fluorescence quantum yield increases proportionately, it equals 0.092 at this temperature. Samples of dyad **1** in the glass at 77 K show emission maxima at 636 and 708 nm, and the quantum yield of fluorescence is $\leq 3 \times 10^{-4}$. These quantum yields allow estimation of the excited singlet state lifetime of **1** as ≤44 ps. This is only an upper limit, as the majority of the emission observed in the steady-state experiment is likely due to minor impurities. This result is consistent with the assignment of the transient absorption, with a lifetime of ~150 ps, to a charge-separated state rather than to the porphyrin first excited singlet state.

Effect of Solvent. Transient absorption studies of dyads **1**–**3** similar to those described above were carried out at ambient temperature in a variety of solvents with widely-differing polarities. In all cases, the transient spectra were characteristic of the porphyrin radical cation of the $P^{\bullet+}-Q^{\bullet-}$ charge-separated state. The rise and decay times, analyzed as exponential processes and deconvoluted from the excitation pulse, are reported in Table 1.

Photoinduced Electron Transfer. The spectroscopic results for dyad **1** may be interpreted with reference to Figure 9, which shows the relevant transient states and interconversion pathways. The energy of the porphyrin first excited singlet state is 1.90 eV, based on the absorption spectrum of **1** and the emission spectrum of model porphyrin **6** (as no emission was observed from the dyad itself). The energy of the charge-separated state, 1.57 eV, is based on the cyclic voltammetric data for **1** in benzonitrile.

In 2-methyltetrahydrofuran, the time-resolved absorption studies at ambient temperature show that excitation of the porphyrin moiety results in ultrafast formation of the $P^{\bullet+}-Q^{\bullet-}$ charge-separated state by photoinduced electron transfer according to step 2 in Figure 9. This conclusion is bolstered by the time-resolved fluorescence studies, which indicate that the lifetime of the porphyrin first excited singlet state is on the order of 1 ps or less, and the steady-state fluorescence quenching, which indicates a lifetime of <5 ps. The rate constant for photoinduced electron transfer can be estimated from eq 1,

$$k_2 = k_{rise} - (1/\tau_o) \quad (1)$$

where k_{rise} is the reciprocal of the rise time of the transient absorption of the porphyrin radical cation (and the reciprocal of the lifetime of the porphyrin first excited singlet state) (Table 1) and τ_o is the lifetime of the first excited singlet state of model porphyrin **6**. For the present case, and indeed for all of the rise times measured for **1**–**3** (Table 1), the quenching is so large that the rate constant for photoinduced electron transfer is equal to k_{rise} within experimental error. Thus, for **1** in 2-methyltetrahydrofuran, k_2 is $\sim 1 \times 10^{12}$ s^{-1}. The rate constants are given to only one significant figure, as the transient absorption data are relatively noisy, and the rise times are close to the width of the laser pulse and must be deconvoluted from it. The lifetime

Table 1. Time Constants for the Rise and Decay of the Charge-Separated State in Porphyrin–Quinone Dyads **1**–**3** as a Function of Solvent

		dyad **1**		dyad **2**		dyad **3**	
solvent	ϵ	k_{rise} (s^{-1})	k_{decay} (s^{-1})	k_{rise} (s^{-1})	k_{decay} (s^{-1})	k_{rise} (s^{-1})	k_{decay} (s^{-1})
benzonitrile	25.60	8×10^{11}	2×10^{11}	3×10^{12}	3×10^{11}	1×10^{12}	2×10^{11}
dichloromethane	9.08	3×10^{12}	5×10^{11}	5×10^{12}	7×10^{11}		
methyltetrahydrofuran	7.60	1×10^{12}	8×10^{10}	5×10^{12}	2×10^{11}	8×10^{11}	7×10^{10}
benzene	2.28	7×10^{12}	4×10^{10}	4×10^{12}	9×10^{10}	2×10^{12}	3×10^{10}
decalin[a]	~2.0			6×10^{12}	5×10^{9}		

[a] This solvent was a ~50:50 mixture of *cis*- and *trans*-decalin.

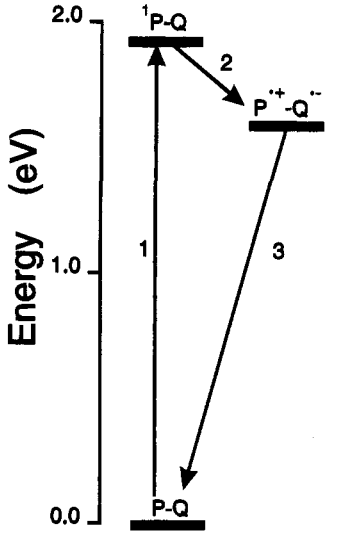

Figure 9. Transient states and interconversion pathways for dyad **1**. The energy of $P^{\bullet+}-Q^{\bullet-}$ is based on cyclic voltammetric measurements in benzonitrile.

of the $P^{\bullet+}-Q^{\bullet-}$ charge-separated state is the reciprocal of the k_{decay} value in Table 1 and equals 13 ps for **1** in 2-methyltetrahydrofuran.

The results in Figures 7 and 8 show that the rate constant for photoinduced electron transfer in **1** is virtually independent of the temperature of the sample over the range 77–298 K; it is $\sim 1 \times 10^{12}$ s^{-1} at all temperatures investigated. This conclusion is supported by the steady-state emission results, which indicate that the maximum lifetime of the porphyrin first excited singlet state at both ambient temperature and 77 K is substantially less than the lifetime of the transient absorption. Thus, this absorption must represent the charge-separated state, rather than the excited singlet state. Charge recombination, on the other hand, slows substantially as the sample is cooled.

The rate constant for photoinduced electron transfer in **1** is also only weakly dependent on solvent polarity (Table 1). The dielectric constants of the solvents investigated range from 25.6 for benzonitrile and 7.6 for 2-methyltetrahydrofuran to 2.28 for benzene, ~2.0 for decalin, and 2.6 for 2-methyltetrahydrofuran at 77 K, but the rate constant for photoinduced electron transfer varies by a factor of less than 10. The lifetime of the charge-separated state depends more strongly on solvent and is longest in the solvents of lowest dielectric constant.

Dyad **3**, in which the double bond in the bridge between the porphyrin and the quinone moieties has been reduced, shows photoinduced electron transfer behavior virtually identical to that observed for **1**. The unsaturation does not substantially alter the electron transfer rate.

The results for zinc dyad **2** follow a trend similar to that observed for **1**. The energy of the first excited singlet state is estimated as ~2.12 eV from the absorption and emission spectra of model porphyrin **7**. The energy of $P_{Zn}^{\bullet+}-Q^{\bullet-}$ in benzonitrile is ~1.39 eV, based on the electrochemical data discussed above. Photoinduced electron transfer at ambient temperature occurs with a rate constant of $\sim 5 \times 10^{12}$ in 2-methyltetrahydrofuran and is virtually independent of solvent. The lifetime of the charge-separated state is more strongly solvent dependent and is 60 times longer in decalin than in benzonitrile (Table 1). Photoinduced electron transfer at 77 K occurs with a rate constant of $\sim 3 \times 10^{12}$ s^{-1}, whereas the charge-recombination rate constant is 1×10^{11} s^{-1}, which is substantially larger than the corresponding value for free base dyad **1**.

Discussion

Thermodynamics of Electron Transfer. In benzonitrile solution, the free energy change for photoinduced electron transfer in dyad **1** is −0.33 eV, as estimated from the cyclic voltammetric studies in this solvent. This estimate contains no corrections for various electrochemical effects such as Coulombic stabilization of an ion by its counterion within the same molecule or by ions of the supporting electrolyte. One popular way to include a correction for the counterion in the dyad and to estimate the free energy change ($\Delta G°$) in other solvents is to use eq 2, which treats the charge-separated state as two spherical

$$\Delta G° = e(E_P - E_Q)_r + \frac{e^2}{4\pi\epsilon_0\epsilon_s}\left[\frac{1}{2R_P} + \frac{1}{2R_Q} - \frac{1}{R_{PQ}}\right] - \frac{e^2}{4\pi\epsilon_0\epsilon_s^r}\left[\frac{1}{2R_P} + \frac{1}{2R_Q}\right] - E_{1P} \quad (2)$$

ions with radii R_P and R_Q separated by a distance R_{PQ} and immersed in a solvent of dielectric constant ϵ_s.[15–17] The quantities E_P and E_Q are the first oxidation and reduction potentials of the porphyrin and quinone, respectively, as measured electrochemically in a reference solvent of dielectric constant ϵ_s^r, ϵ_0 is the permittivity of free space, E_{1P} is the energy of the porphyrin first excited singlet state, and e is the electronic charge.

The application of eq 2 requires a knowledge of the center-to-center distance between the porphyrin and quinone radical ions in the charge-separated state (nominally 6.7 Å) and the radius of each ion. The radii are somewhat problematical, as the ions are certainly not spherical. However, eq 2 has been shown by Wasielewski and co-workers[17] to be applicable to a set of porphyrin–quinone dyads when R_P and R_Q are 5 and 3 Å, respectively. Using these values, the free energy change for the electron transfer reaction in **1** is estimated to be −0.41 eV in benzonitrile. In 2-methyltetrahydrofuran (ϵ = 7.60), eq 2 yields a free energy change of −0.26 eV, which is still reasonably exergonic. In benzene (ϵ = 2.28) and a 2-methyltetrahydrofuran glass at 77 K (ϵ = 2.60),[18] eq 2 gives free energy

(15) Weller, A. *Z. Phys. Chem. (Munich)* **1982**, *133*, 93–98.
(16) Schmidt, J. A.; Liu, J.-Y.; Bolton, J. R.; Archer, M. D.; Gadzekpo, V. P. Y. *J. Chem. Soc., Faraday Trans. 1* **1989**, *85*, 1027–1041.
(17) Gaines, G. L., III; O'Neil, M. P.; Svec, W. A.; Niemczyk, M. P.; Wasielewski, M. R. *J. Am. Chem. Soc.* **1991**, *113*, 719–721.
(18) Furutsuka, T.; Imura, T.; Kojima, T.; Kawabe, K. *Eng. Rep. Osaka Univ.* **1974**, *24*, 367.

change values of 0.261 and 0.170 for **1** using the parameters listed above. These estimates are clearly incorrect, as reactions with positive free energy changes of this magnitude could not occur at the relevant rates and temperatures.

This lack of agreement with experiment is not surprising, as the ions in the dyad are not spherical, their "radii" are uncertain, their separation is also uncertain (the π-electron systems are large and polarizable, so that Coulombic attraction could reduce the separation of the centers of charge), and the separation of charge is likely less than the sum of the ionic radii. Moreover, as the solvent dielectric constant is reduced, two effects come into play: loss of solvent stabilization of the ions and increased stabilization by mutual Coulombic attraction. Therefore, eq 2 can yield a large range of energies for reasonable estimates of R_P, R_Q, and R_{PQ}. Depending upon the choice of parameters, $\Delta G°$ can increase, decrease, or remain the same as the solvent dielectric constant decreases. The application of eq 2 to the solvent dependence of $\Delta G°$ in porphyrin−quinone dyads has been questioned by other investigators.[16] Thus, the results of calculations using eq 2 are most useful as a framework for discussion, rather than as reliable estimates.

These considerations suggest that it might be more appropriate to treat the charge-separated state in the dyads as a single dipole in a cavity surrounded by solvent.[19-22] This treatment can also give reasonable estimates of the energies of the charge-separated states in different solvents if suitable parameters are employed. However, as with eq 2, the results of the calculation depend strongly upon the values chosen for the various parameters such as cavity radius, for which reliable estimates are not available.

The electrochemical and spectroscopic data applicable to zinc dyad **2** yield an estimate of 1.39 eV for the energy of $P_{Zn}^{\bullet+}$−$Q^{\bullet-}$, and an uncorrected driving force of −0.73 eV for photoinduced electron transfer in benzonitrile. Application of eq 2 to this molecule using the parameters mentioned above gives $\Delta G°$ values of −0.81, −0.66, −0.14, and −0.23 eV in benzonitrile, 2-methyltetrahydrofuran, benzene, and the organic glass at 77 K, respectively.

Kinetics of Electron Transfer. A useful and often-employed starting point for the discussion of electron transfer reactions in porphyrin−quinone dyads is eq 3, which was developed for

$$k_{et} = \sqrt{(\pi/\hbar^2\lambda k_B T)}|V|^2 \exp[-(\Delta G° + \lambda)^2/4\lambda k_B T] \quad (3)$$

nonadiabatic electron transfer reactions.[23-25] The electron transfer rate constant is k_{et}. The pre-exponential factor includes the electronic matrix element V that describes the coupling of the reactant state with that of the product. In addition to Planck's constant $\hbar$, Boltzmann's constant k_B, and the absolute temperature T, this factor also includes the reorganization energy for the reaction, λ. The reorganization energy is associated with the nuclear motions necessary to carry the molecule from the initial to the final state. It is convenient to express λ as the sum of a solvent-independent term λ_i, which originates from internal molecular structural differences between the reactant and product, and λ_s, the solvent reorganization energy, which is due to differences in the orientation and polarization of solvent molecules around the neutral ground state and the zwitterionic charge-separated state.

It will be noted that eq 3 predicts an increase in rate with thermodynamic driving force (the "normal" region), up to a maximum when $-\Delta G° = \lambda$, and a decrease in rate as the standard free energy change becomes more negative in the "inverted" region. At the maximum, the activation barrier for the reaction disappears.

In dyads **1**−**3**, the photoinduced electron transfer rate constant is nearly independent of solvent, temperature, and free energy change. Thus, accommodation of the results within the framework of eq 3 requires a number of qualifying and perhaps unlikely assumptions, as illustrated below.

Solvent Effects. Equation 3 predicts that the electron transfer rate constant will depend strongly upon thermodynamic driving force. As shown in eq 2, $\Delta G°$, and therefore k_{et}, are expected to vary with solvent. However, the rate constants for **1** and **2** change very little on going from a nonpolar solvent such as benzene or decalin to a very polar species such as benzonitrile. A possible explanation for this effect lies in the fact that the reorganization energy λ is also a function of the solvent. Marcus has proposed that λ_s depends on the static (ϵ_s) and high-frequency ($\epsilon_{op} = n^2$) dielectric constants of the solvent as shown in eq 4.[16,26,27] For many reasonable combinations of R_P, R_Q,

$$\lambda_s = \frac{e^2}{4\pi\epsilon_0}\left(\frac{1}{2R_P} + \frac{1}{2R_Q} - \frac{1}{R_{PQ}}\right)\left(\frac{1}{\epsilon_{op}} - \frac{1}{\epsilon_s}\right) \quad (4)$$

and R_{PQ} in the dyads, eqs 2 and 4 predict that changes in $\Delta G°$ and λ_s with solvent will tend to compensate one another in eq 3 so that $(\Delta G° + \lambda)$ and therefore the electron transfer rate constant do not vary much. This partial cancellation of effects has been noted previously for other systems.[12,28] Thus, the relatively weak dependence of electron transfer rates in each dyad on solvent can be accommodated within the framework of eq 3 if suitable molecular parameters are selected.

Effect of Temperature. In the 77−295 K range, temperature has essentially no effect on photoinduced electron transfer rates in the dyads and the activation energy for electron transfer is very small. Although this result for dyad **1** is in general inconsistent with eq 3, it may be rationalized if $-\Delta G°$ equals λ at all temperatures so that the exponential term in eq 3 approaches unity and the electron transfer rate is maximal. This is unlikely. The internal reorganization energy λ_i for porphyrin−quinone dyads has been estimated as ~0.3 eV.[12,29,30] Thus, the required equality could occur only if $-\Delta G°$ happens to always equal $(\lambda_s + 0.3)$ eV as the solvent dielectric constant changes from 2.60 at 77 K to 7.60 at ambient temperatures.

Effect of Free Energy Change. Equation 3 suggests that the 0.4 eV difference in $\Delta G°$ between **1** and **2** should lead to a substantial difference in photoinduced electron transfer rate constant under similar conditions of solvent, temperature, etc. In other porphyrin−quinone systems, a comparable difference in $\Delta G°$ in the normal region is accompanied by changes in rate of ~100−1000.[12] Table 1 shows that the rate difference for **1** and **2** is a factor of about 4 or less. Barring a fortuitous situation wherein **1** and **2** fall in the normal and inverted regions, respectively, and happen to share the same rate constant in all

(19) Heitele, H.; Pöllinger, F.; Kremer, K.; Michel-Beyerle, M. E.; Futscher, M.; Voit, G.; Weiser, J.; Staab, H. A. *Chem. Phys. Lett.* **1992**, *188*, 270−278.
(20) Lippert, E. *Z. Naturforsch.* **1955**, *10a*, 541.
(21) Onsager, L. *J. Am. Chem. Soc.* **1936**, *58*, 1486−1493.
(22) Seely, G. R. In *Current Topics in Bioenergetics*; Sanadi, D. R., Vernon, L. P., Eds.; Academic Press: New York, 1978; pp 3−37.
(23) Marcus, R. A. *J. Chem. Phys.* **1956**, *24*, 966−978.
(24) Marcus, R. A.; Sutin, N. *Biochim. Biophys. Acta* **1985**, *811*, 265−322.
(25) Levich, V. O. *Adv. Electrochem. Electrochem. Eng.* **1966**, *4*, 249−371.
(26) Marcus, R. A. *Can. J. Chem.* **1959**, *37*, 155−163.
(27) Marcus, R. A. *J. Chem. Phys.* **1965**, *43*, 679−701.
(28) Kroon, J.; Verhoeven, J. W.; Paddon-Row, M. N.; Oliver, A. M. *Angew. Chem., Int. Ed. Engl.* **1991**, *30*, 1358−1361.
(29) Joran, A. D.; Leland, B. A.; Felker, P. M.; Zewail, A. H.; Hopfield, J. J.; Dervan, P. B. *Nature (London)* **1987**, *327*, 508−511.
(30) Heitele, H.; Pöllinger, F.; Häberle, T.; Michel-Beyerle, M. E.; Staab, H. A. *J. Phys. Chem.* **1994**, *98*, 7402−7410.

solvents and at all temperatures, the behavior of the dyads is not in agreement with eq 3 and not typical of the majority of porphyrin–quinone systems studied to date.

As mentioned above, the temperature effect for free-base dyad **1** is consistent with eq 3 if $-\Delta G^\circ = \lambda$ for this molecule at all temperatures in 2-methyltetrahydrofuran. If this were the case, zinc dyad **2** would necessarily fall significantly into the inverted region and the electron transfer rate should be *slower* for **2** than for **1**, whereas in fact, it is the same or faster (Table 1). Semiclassical refinements of eq 3 which take into account quantized vibrational states of the acceptor do show a somewhat less-pronounced falloff of rate with increasing driving force in the inverted region[31,32] but do not eliminate inverted behavior. It will be noted that **2** is a zinc-containing dyad, whereas **1** is a free base. There is evidence from two other series of porphyrin–quinone dyads that zinc porphyrin-containing dyads with high driving forces feature very high rates of photoinduced electron transfer and may not demonstrate inverted behavior.[10,30] In this regard, zinc-containing porphyrin dyads have recently been found to feature photoinduced electron transfer in the normal region that falls on a rate-vs-free energy curve different from that of free-base analogs.[33]

Effect of Electronic Coupling. The perturbation of the porphyrin absorption spectra of **1** and **2** resulting from linkage to the quinone suggests significant mixing of the π-electron systems of the two moieties. This interaction likely occurs across the bicyclic bridge joining them, as the π-electron systems are in closest proximity in this region. For example, the participation of the carbon–carbon double bond in the solvolysis of norbornene derivatives has been much discussed.[34] In addition, separation of two π-electron systems by two single bonds in related norbornyl[11] and triptycyl[35] bridging groups has been found to allow significant electronic coupling between electron donor and acceptor units. In this connection, it is interesting to note that, when the double bond in the bicyclic bridge of dyad **1** is removed by reduction to yield **3**, the rate constant for photoinduced electron transfer does not change significantly.

The electronic interaction between the donor and acceptor is of interest because it determines the electronic coupling V in eq 3. The rapid photoinduced electron transfer in the dyads suggests that V may be relatively large, so that it approaches thermal energies (for example, at 295 K, k_BT ~200 cm^{-1}, or ~0.025 eV). A rough indication of the coupling in the dyads may be obtained by assigning a value of unity to the exponential term in eq 3. In this case, an electron transfer rate constant of 5×10^{12} s^{-1} yields a value of ~100 cm^{-1} for V at room temperature with typical values of λ (~0.5 eV).

The observation that photoinduced electron transfer rate constants in the dyads are approaching nuclear vibrational frequencies (10^{12}–10^{14} s^{-1}) raises the prospect that the rate of electron transfer may be controlled mainly by intramolecular nuclear vibrations along the coordinate that carries reactants into products. If this is the case, it can explain the lack of sensitivity to environmental factors noted above. It is clear from the experimental results that even with a small thermodynamic driving force, at low temperatures in a rigid, nonpolar solvent, photoinduced electron transfer in dyad **1** occurs at rates approaching the frequencies of nuclear vibrations. Changing conditions in order to make electron transfer more "favorable" (e.g., raising the temperature or making ΔG° more negative by metalation of the porphyrin) cannot increase the rate substantially. It is already occurring at close to the limiting rate. (In this connection, it should be noted that, if nuclear vibrations are controlling electron transfer rates, eq 3, developed for nonadiabatic transfer, can only yield estimates for the electronic coupling, V.)

The theoretical possibility of long-range, solvent-independent photoinduced electron transfer in linked donor–acceptor systems has been discussed by Jortner *et al.*[36] This "molecular limit" for electron transfer requires relatively large electronic coupling, V, and is envisioned as a radiationless transition having Franck–Condon factors arising from intramolecular vibrational overlaps. The lack of sensitivity to external factors noted for photoinduced electron transfer in **1**–**3** is consistent with electron transfer as an essentially intramolecular relaxation process of this kind.

Solvation Dynamics. Solvent motions can in principle control the rates of photoinduced electron transfer.[37–42] Many solvents show a distribution of relaxation times. "Average" relaxation times for solvents such as those used in this study are on the order of a few picoseconds. For example, two relaxation times of 2.1 and 6.1 ps have been observed for benzonitrile at 298 K. Clearly, at least some solvent motions are substantially slower than photoinduced electron transfer in the dyads. The data in Table 1 provide no compelling evidence for an effect of solvent dynamics on electron transfer rate constants. For example, the rate in 2-methyltetrahydrofuran glass at 77 K, where many solvent motions are presumably slow, is essentially identical to the rates in polar or nonpolar solvents at ambient temperature. This suggests that, to the extent that nuclear reorganization plays a role in promoting electron transfer in the dyads, this reorganization involves mainly internal vibrational modes of the molecule. To the degree that electron transfer does not require solvent reorganization, it will be independent of the solvent dielectric constant and solvent relaxation times, as observed in the dyads. On the other hand, reorientation of solvent dipoles will still stabilize the $P^{\bullet+}$–$Q^{\bullet-}$ charge-separated state when the lifetime of that state is substantially longer than the solvent relaxation times (Table 1).

Nuclear Tunneling. One of the consequences of quantum formulations of electron transfer theory is that electron transfer may occur by nuclear tunneling from the reactant to the product potential energy surface. Such tunneling is effective only if the required nuclear displacements are small and would be favored by small reorganization energies such as might be found in the rigid porphyrin–quinone systems, especially in viscous, nonpolar solvents. The usual evidence for nuclear tunneling, rapid, temperature-dependent electron transfer at higher temperatures and slower, temperature-independent transfer at lower temperatures, is not observed in the dyads. Indeed, as discussed above, there appears to be little or no barrier to electron transfer in these molecules.

Sample Temperature. In the transient absorption experiments, the samples were excited by laser pulses that populate

(31) Jortner, J. *J. Chem. Phys.* **1976**, *64*, 4860–4867.
(32) Jortner, J. *J. Am. Chem. Soc.* **1980**, *102*, 6676–6686.
(33) DeGraziano, J. M.; Liddell, P. A.; Leggett, L.; Moore, A. L.; Moore, T. A.; Gust, D. *J. Phys. Chem.* **1994**, *98*, 1758–1761.
(34) March, J. *Advanced Organic Chemistry*; Wiley-Interscience: New York, 1992; pp 314–316.
(35) Wasielewski, M. R.; Niemczyk, M. P.; Svec, W. A.; Pewitt, E. B. *J. Am. Chem. Soc.* **1985**, *107*, 1080–1082.
(36) Jortner, J.; Bixon, M.; Heitele, H.; Michel-Beyerle, M. E. *Chem. Phys. Lett.* **1992**, *197*, 131–135.
(37) Barbara, P. F.; Jarzeba, W. *Adv. Photochem.* **1990**, *15*, 1–66.
(38) Heitele, H. *Angew. Chem., Int. Ed. Engl.* **1993**, *32*, 359–377.
(39) Harrison, R. J.; Pearce, B.; Beddard, G. S.; Cowan, J. A.; Sanders, J. K. M. *Chem. Phys.* **1987**, *116*, 429–448.
(40) van der Zwan, G.; Hynes, J. T. *J. Phys. Chem.* **1985**, *89*, 4181–4188.
(41) Calef, D. F.; Wolynes, P. G. *J. Phys. Chem.* **1983**, *87*, 3387–3400.
(42) Zaleski, J. M.; Chang, C. K.; Leroi, G. E.; Cukier, R. I.; Nocera, D. G. *J. Am. Chem. Soc.* **1992**, *114*, 3564–3565.

upper vibrational levels of the porphyrin first excited singlet state. The excess energy from these pulses is eventually dissipated into the lattice. However, it is conceivable that this may occur on a time scale comparable to or longer than the observed times for photoinduced electron transfer.[43,44] It has been reported that excitation of some porphyrins in solution at ambient temperatures is followed by relaxation processes within the excited singlet state manifold that can be tracked by their effect upon transient absorption spectra. This vibrational relaxation can require several picoseconds.[43] In this study, the transient absorption of the first excited singlet state of model porphyrin **6** in the 630−640 nm region rises with a time constant of 0.26 ps and there is no evidence for slower processes. A study of electron transfer in the dyads as a function of excitation wavelength would help address this question.

The low-temperature studies may be susceptible to similar effects related to the rate of dissipation of excess energy from the laser pulse, and therefore in some respects, electron transfer may not be occurring at the bath temperature.[44] If this is indeed a factor in this study, it may also be a factor in many other investigations, including those of natural photosynthetic photoinduced electron transfer, which occurs in a few picoseconds.

Optical Electron Transfer. Electron transfer can occur by an optical transition from the ground state directly into an absorption band of a charge-transfer state. The charge-separated state thus formed subsequently relaxes via internal and solvent nuclear motions. The very rapid electron transfer in the dyads requires consideration of this possibility. Indeed, under some conditions, the electron transfer rate constant in Table 1 is comparable to the reciprocal of the experimental rise time of the excited singlet state of the model porphyrin (i.e., the ~200-fs width of the excitation pulse). However, in other cases, the rise of the porphyrin radical cation absorption is substantially slower than this (see, for example, Figure 6). Assuming that these longer rise times do indeed reflect the electron transfer event, optical electron transfer is not occurring. The perturbations in the absorption spectra of the dyads relative to model porphyrins (Figure 2) could be explained in part by the presence of a broad but very weak charge-transfer band beneath the porphyrin Q-bands. However, the absorption spectra are essentially unaffected by solvent. To the extent that the charge-separated state is stabilized by solvent, one would expect the spectrum of any charge-transfer absorption to be a function of solvent.

Charge Recombination. Charge recombination of $P^{\bullet+}-Q^{\bullet-}$ (step 3 in Figure 9) differs from photoinduced electron transfer in that it involves a different set of electronic states and energies, molecular orbitals, and time scales. Thus, it need not show similar behavior. For example, photoinduced electron transfer occurs from the porphyrin LUMO, which has significant orbital density on both carbon atoms bearing the bridge to the quinone, whereas charge recombination involves the porphyrin HOMO, which has little orbital density at the porphyrin *meso* carbons.[45]

Effects of strong electronic coupling on electron transfer in the normal and Marcus inverted regimes will be different.[46-49] Increasing the electronic coupling, V, in the normal region of eq 3 leads to adiabatic electron transfer which occurs on a single energy surface. It also lowers the activation barrier for transfer. In the inverted region, electron transfer always involves two different potential surfaces, and increasing the electronic coupling increases the width of the avoided crossing between the reactant and product surfaces. Thus, in the normal region, increased electronic coupling increases electron transfer rate constants and decreased coupling decreases rates. In the inverted region, electron transfer rates will be slowed in both the weak coupling and strong coupling limits.

Given these considerations, it is not surprising to find that charge recombination in the dyads has different characteristics from charge separation (Table 1). For example, charge recombination is substantially slower than charge separation (which is not the case in many other porphyrin−quinone systems[50]). In nonpolar solvents, the difference in rate constants is large. Charge recombination in **2** dissolved in decalin is more than 1000 times slower than charge separation. Charge recombination rates in the dyads should therefore not be subject to possible effects due to solvent reorientation on the electron transfer time scale, vibrational relaxation, or incomplete thermal equilibration.

How, then, do we think about charge recombination in the dyads? It will be noted from the discussion of thermodynamics that the free energy change for charge recombination is very large (up to about −1.9 eV for **1** in benzene). This is far into the inverted region of eq 3, as reorganization energies for porphyrin−quinone systems in organic solvents are typically ~1 eV.[1,6-10] Inverted behavior is consistent with the relatively slow rates observed for charge recombination. It is also consistent with the observation that charge recombination is slightly faster for **2** than for **1** in all solvents. The driving force for recombination is greater for free base **1** than for zinc dyad **2**, and in the inverted region, a larger driving force leads to a slower rate. The same phenomenon is seen at 77 K, where recombination rates for **2** are again larger than those for **1**. The recombination rates also slow as the solvent dielectric constant decreases (Table 1). Again, this may be ascribed to inverted behavior. As the solvent dielectric constant decreases, λ_s and solvent stabilization of $P^{\bullet+}-Q^{\bullet-}$ are reduced. This leads to a decrease in electron transfer rate. Finally, the charge recombination rate decreases as the temperature is reduced (Figure 8). This result is in accord with thermally activated behavior (eq 3) and with a decrease in the effective dielectric constant of the solvent as it becomes viscous.

Comparison with Other Porphyrin−Quinone Systems. As mentioned in the introduction, the vast majority of the porphyrin−quinone systems studied to date display relatively slow, nonadiabatic photoinduced electron transfer whose rate is a strong function of solvent, temperature, and driving force.[1,6-10] For example, data for photoinduced charge separation in a porphyrin-benzoquinone system are available for 16 solvents, binary solvent mixtures, and various temperatures. These data are reasonably well correlated with Marcus theory if specific solvent interactions and the solvent dependence of λ and ΔG° are correctly taken into account.[16,51-53] There are, however, a few classes of these dyads that demonstrate relatively strong electronic coupling and/or very rapid electron transfer rates.

Several groups have reported porphyrin−quinone dyads in which a quinone moiety replaces a *meso*-aryl group of a

(43) Rodriguez, J.; Holten, D. *J. Chem. Phys.* **1989**, *91*, 3525−3531.
(44) Bolton, J. R.; Archer, M. D. *J. Phys. Chem.* **1991**, *95*, 8453−8461.
(45) Spangler, D.; Maggiora, G. M.; Shipman, L. L.; Christoffersen, R. E. *J. Am. Chem. Soc.* **1977**, *99*, 7470−7477.
(46) Marcus, R. A. *J. Chem. Phys.* **1970**, *52*, 2803−2804.
(47) Netzel, T. L.; Bergkamp, M. A.; Chang, C. K. *J. Am. Chem. Soc.* **1982**, *104*, 1952−1957.
(48) Cave, R. J.; Siders, P.; Marcus, R. A. *J. Phys. Chem.* **1986**, *90*, 1436−1444.
(49) Cukier, R. I.; Nocera, D. *J. Chem. Phys.* **1992**, *97*, 7371−7376.
(50) Hung, S.-C.; Lin, S.; Macpherson, A. N.; DeGraziano, J. M.; Kerrigan, P. K.; Liddell, P. A.; Moore, A. L.; Moore, T. A.; Gust, D. *J. Photochem. Photobiol. A: Chem.* **1994**, *77*, 207−216.
(51) Schmidt, J. A.; Siemiarczuk, A.; Weedon, A. C.; Bolton, J. R. *J. Am. Chem. Soc.* **1985**, *107*, 6112−6114.
(52) Liu, J.-Y.; Schmidt, J. A.; Bolton, J. R. *J. Phys. Chem.* **1991**, *95*, 6924−6927.
(53) Liu, J. Y.; Bolton, J. R. *J. Phys. Chem.* **1992**, *96*, 1718−1725.

tetraarylporphyrin.[54-61] In these molecules, the quinone is formally conjugated to the porphyrin ring, and interaction of the two π-electron systems is limited only by the degree of twisting of the quinone out of the porphyrin plane. Some of these systems show significant perturbation of their absorption spectra and rapid electron transfer quenching of the porphyrin first excited singlet state. In one of these systems, wherein a porphyrin dyad bears a quinone electron acceptor, rapid photoinduced electron transfer at low temperatures has been reported.[57-61] In a second, charge-transfer emission from a charge-separated state was observed.[56] There is evidence that, in this class of molecules, rotations about the single linkage bond may rapidly modulate electronic coupling.[62]

A second class of strongly coupled porphyrin–quinone systems comprises cyclophanes, where the quinone is "strapped" across the face of the porphyrin by two or more linkages containing single bonds.[19,30,38,63-71] These molecules can in principle achieve strong electronic coupling through a face-to-face arrangement of the porphyrin and quinone, although the flexibility of the linkages between the two moieties sometimes leads to conformational heterogeneity. Some of these systems demonstrate only a very weak dependence of the rate of photoinduced electron transfer on solvent and temperature, much as is observed for **1–3**. For example, a cyclophane system examined by Mauzerall and co-workers[64,65] undergoes photoinduced electron transfer with rate constants about 1000 times slower than observed for **1–3**. However, the dependence on solvent and temperature is weak (an effect attributed to nonadiabatic electron tunneling[64,65]). Analysis of the results is somewhat complex because the flexible linkages allow two conformers with significant populations.

A group of researchers from Heidelberg and Munich have recently studied a series of cyclophane systems.[19,30,38,63-71] Dyads with relatively low driving force for electron transfer in polar solvents (comparable to **1**) show relatively slow photoinduced electron transfer in nonpolar solvents and significantly faster transfer in polar solvents. For a few molecules with large negative $\Delta G°$ values, photoinduced electron transfer occurs in about 1 ps in all solvents investigated and at low temperatures. Exact transfer rate constants are unavailable because of instrumental limitations, but it is clear that the behavior of these cyclophanes is similar in many respects to that of dyads **1–3**. In these cases as well, electron transfer rate constants appear to be determined mainly by internal molecular vibrations, rather than external factors, and may be approaching the "molecular limit."[30,36] The charge recombination rates in these molecules also appear to be insensitive to solvent, unlike those observed for **1–3**. However, this interpretation may be complicated by conformational heterogeneity arising from flexibility in the porphyrin–quinone linkage. More rigid analogs of these cyclophanes may help resolve these questions.

Porphyrin–quinone electron transfer at relatively low temperatures has been observed in a few systems in which electron transfer rates are substantially slower than those observed for **1–3**. In one case, where the moieties are linked through a bicyclooctylphenyl spacer, a weak temperature dependence for the initial rate of photoinduced electron transfer allows transfer to occur even at 77 K, although the decays are strongly multiexponential at low temperatures due to slow conformational interconversion by rotations about single bonds in the linkage.[72,73] As mentioned above, dyads with a large thermodynamic driving force for electron transfer in polar solvents at ambient temperatures can preserve enough driving force at low temperatures to undergo rapid photoinduced electron transfer even at 77 K.[12,17]

Comparison with Photosynthesis. The insensitivity of photoinduced electron transfer in **1–3** to driving force and environmental effects such as solvent and temperature is shared by photosynthetic reaction centers.[1-5] In bacterial reaction centers, photoinduced electron transfer occurs on the picosecond time scale even at 4 K. It happens in a membrane–protein matrix which is considerably less fluid than solutions at ambient temperature and rigid at liquid helium temperatures. Although $\Delta G°$ cannot be varied over as large a range as in model systems, the sensitivity of photoinduced electron transfer to changes in driving force is apparently very small. Recently, kinetic and thermodynamic data for the initial electron transfer step in bacterial photosynthesis has been interpreted in terms of a strongly coupled system which approaches the adiabatic limit.[4,5]

Conclusions

As discussed above, ultrafast photoinduced electron transfer that is only weakly dependent on temperature, solvent, and driving force has been observed in the rigid porphyrin–quinone dyads. Electron transfer in these molecules is apparently controlled by intramolecular vibrations, either through vibrational overlap terms viewed in the context of radiationless transition theory, or as limiting factors in the conversion of reactant to product on a quasi-adiabatic potential surface. In contrast to the behavior of the photoinduced electron transfer rate constant, charge recombination in the dyads is relatively sensitive to thermodynamic and environmental factors and is qualitatively in accord with Marcus theory. This fact suggests that rigid dyads of this general type might be excellent candidates for incorporation into more complex constructs for solar energy conversion or opto-electronic purposes. In many triads and other molecular devices, recombination of the initially formed charge-separated state is very rapid[50] and devising fruitful secondary electron transfer reactions that compete successfully with charge recombination is a significant chal-

(54) Bergkamp, M.; Dalton, J.; Netzel, T. *J. Am. Chem. Soc.* **1982**, *104*, 253–259.
(55) Cormier, R. A.; Posey, M. R.; Bell, W. L.; Fonda, H. N.; Connolly, J. S. *Tetrahedron* **1989**, *45*, 4831–4843.
(56) Kamioka, K.; Cormier, R. A.; Lutton, T. W.; Connolly, J. S. *J. Am. Chem. Soc.* **1992**, *114*, 4414–4415.
(57) Rodriguez, J.; Kirmaier, C.; Johnson, M. R.; Friesner, R. A.; Holten, D.; Sessler, J. L. *J. Am. Chem. Soc.* **1991**, *113*, 1652–1659.
(58) Sessler, J. L.; Piering, S. *Tetrahedron Lett.* **1987**, *28*, 6569–6572.
(59) Sessler, J. L.; Johnson, M. R.; Lin, T.-Y.; Creager, S. E. *J. Am. Chem. Soc.* **1988**, *110*, 3659–3661.
(60) Sessler, J. L.; Johnson, M. R.; Creager, S. E.; Fettinger, J. C.; Ibers, J. A. *J. Am. Chem. Soc.* **1990**, *112*, 9310–9329.
(61) Sessler, J. L.; Capuano, V. L. *Angew. Chem., Int. Ed. Engl.* **1990**, *29*, 1134–1137.
(62) Fonda, H. N.; Gilbert, J. V.; Cormier, R. A.; Sprague, J. R.; Kamioka, K.; Connolly, J. S. *J. Phys. Chem.* **1993**, *97*, 7024–7033.
(63) Lindsey, J. S.; Mauzerall, D. C.; Linschitz, H. *J. Am. Chem. Soc.* **1983**, *105*, 6528–6529.
(64) Lindsey, J. S.; Delaney, J. K.; Mauzerall, D. C.; Linschitz, H. *J. Am. Chem. Soc.* **1988**, *110*, 3610–3621.
(65) Delaney, J. K.; Mauzerall, D. C.; Lindsey, J. S. *J. Am. Chem. Soc.* **1990**, *112*, 957–963.
(66) Leighton, P.; Sanders, J. K. M. *J. Chem. Soc., Chem. Commun.* **1985**, 24–25.
(67) Irvine, M. P.; Harrison, R. J.; Beddard, G. S.; Leighton, P.; Sanders, J. K. M. *Chem. Phys.* **1986**, *104*, 315–324.
(68) Osuka, A.; Furuta, H.; Maruyama, K. *Chem. Lett.* **1986**, 479–482.
(69) Frey, W.; Klann, R.; Laermer, F.; Elsaesser, T.; Baumann, E.; Futscher, M.; Staab, H. A. *Chem. Phys. Lett.* **1992**, *190*, 567–573.
(70) Pöllinger, F.; Heitele, H.; Michel-Beyerle, M. E.; Anders, C.; Futscher, M.; Staab, H. A. *Chem. Phys. Lett.* **1992**, *198*, 645–652.
(71) Scherer, P. O. J.; Fischer, S. F. *Chem. Phys. Lett.* **1992**, *190*, 574–580.
(72) Khundkar, L. R.; Perry, J. W.; Hanson, J. E.; Dervan, P. B. *J. Am. Chem. Soc.* **1994**, *116*, 9700–9709.
(73) Leland, B. A.; Joran, A. D.; Felker, P. M.; Hopfield, J. J.; Zewail, A. H.; Dervan, P. B. *J. Phys. Chem.* **1985**, *89*, 5571–5573.

lenge. In the rigid dyads, charge recombination rates may be varied over a wide range by alteration of thermodynamic and environmental factors, whereas these same factors do not reduce the rate (or quantum yield) of the photoinduced electron transfer event. Thus, these systems would seem to offer considerable design flexibility to the molecular engineer, although the strong interactions between the ions in the charge-separated state must be taken into consideration.

Experimental Section

Synthesis. The preparation of model porphyrins **6** and **7** has been reported.[13,74] Porphyrin diene **4** was synthesized as described previously for a closely-related analog:[13] ^{1}H NMR (500 MHz, $CDCl_3$) δ −1.79 (1H, s, NH), −1.45 (1H, s, NH), 1.12 (3H, t, J = 8 Hz, 12-CH_2CH_3), 1.18 (3H, t, J = 8 Hz, 8-CH_2CH_3), 2.67 (2H, q, J = 8 Hz, 12-CH_2-CH_3), 2.88 (2H, q, J = 8 Hz, 8-CH_2CH_3), 3.50 (3H, s, 13-CH_3), 3.67 (3H, s, 7-CH_3), 3.69 (3H, s, 17-CH_3), 3.78 (3H, s, 18-CH_3), 4.02 (3H, s, 3-CH_3), 4.14 (3H, s, $COOCH_3$), 7.94 (1H, m, 2^2-H), 8.01 (1H, m, 2^3-H), 8.29 (2H, d, J = 8 Hz, 10Ar2,6-H), 8.36 (2H, d, J = 8 Hz, 10Ar3,5-H), 9.13 (1H, d, J = 10 Hz, 2^1-H), 9.99 (1H, d, J = 12 Hz, 2^4-H), 10.34 (1H, s, 15-H), 10.50 (1H, s, 5-H); MS (FAB) m/z 621.3226 (calcd for $(M + H)^+$, 621.3229); UV/vis (CH_2Cl_2) 236, 317, 414, 542, 586, 606, 662 nm.

In order to prepare dyad **1**, a heavy-walled glass ampoule containing 75 mg (0.12 mmol) of diene **4**, 1.5 g of naphthoquinone, and 8 mL of 1,2-dichlorobenzene was sealed under a nitrogen atmosphere and heated to 176 °C for 5 h. After the tube was allowed to cool, it was opened and the solvent was removed by distillation at reduced pressure. Chromatography of the residue on silica gel (toluene containing 1.0−1.5% ethyl acetate) gave 68 mg of **1** (72%): ^{1}H NMR (500 MHz, $CDCl_3$) δ −2.21 (1H, s, NH), −1.99 (1H, s, NH), 1.09 (3H, t, J = 8 Hz, 12-CH_2CH_3), 1.11 (3H, t, J = 8 Hz, 8-CH_2CH_3), 2.59 (2H, q, J = 8 Hz, 12-CH_2CH_3), 2.71 (2H, q, J = 8 Hz, 8-CH_2CH_3), 3.41 (3H, s, 13-CH_3), 3.49 (3H, s, 7-CH_3), 3.65 (3H, s, 3-CH_3), 3.68 (3H, s, 17-CH_3), 4.10 (3H, s, $COOCH_3$), 4.13 (3H, s, 18-CH_3), 6.23 (1H, dd, J = 6, 1 Hz, 2^1-H), 7.34 (1H, ddd, J = 7, 7, 1 Hz, 2^2-H), 7.53 (1H, ddd, J = 7, 7, 1 Hz, QH), 7.57 (1H, ddd, J = 7, 7, 1 Hz, QH), 7.63 (1H, ddd, J = 7, 7, 1 Hz, 2^3-H), 7.91 (1H, m, 2^4-H), 7.93 (1H, m, QH), 8.07 (1H, dd, J = 7, 1 Hz, QH), 8.17 (1H, dd, J = 8, 1 Hz, 10Ar6-H), 8.25 (1H, dd, J = 8, 1 Hz, 10Ar2-H), 8.31 (1H, dd, J = 8, 1 Hz, 10Ar5-H, 8.33 (1H, dd, J = 8, 1 Hz, 10Ar3-H), 9.98 (1H, s, 5-H), 10.04 (1H, s, 15-H); MS (FAB) m/z 777.3436 (calcd for $(M + H)^+$, 777.3440); UV/vis (CH_2Cl_2) 245, 410, 508, 590, 646 nm. Zinc analog **2** was prepared in quantitative yield by stirring a solution of **1** in dichloromethane with an excess of zinc acetate for 0.5 h, distilling the solvent at reduced pressure, and purifying the product by thin-layer chromatography on silica gel.

Dyad 3. A mixture of dyad **2** (10 mg, 0.026 mmol) and 10% palladium on charcoal (10 mg) in 15 mL of ethyl acetate was stirred under a hydrogen atmosphere (40 psi) for 2 h. The catalyst was then separated by filtration, and the solvent was removed by distillation at reduced pressure to produce crude dyad **5**. This material was dissolved in 6 mL of dichloromethane and stirred with trifluoroacetic acid (0.3 mL) to remove the coordinated zinc. After 20 min, the green reaction mixture was neutralized with aqueous sodium bicarbonate and the organic phase was dried over sodium sulfate. After filtration, the solvent was distilled under reduced pressure and the residue was chromatographed on silica gel (dichloromethane containing 0.5% acetone) to give **3** (7.8 mg, 84%): ^{1}H NMR (500 MHz, $CDCl_3$) δ −2.33 (1H, brs, NH), −2.27 (1H, brs, NH), 1.12 (3H, t, J = 8 Hz, 12-CH_2CH_3), 1.14 (3H, t, J = 8 Hz, 8-CH_2CH_3), 2.79 (6H, m, 2^2-CH_2, 8-CH_2CH_3, 12-CH_2CH_3), 2.96 (1H, m, 2^3-H), 3.06 (1H, m, 2^3-H), 3.47 (3H, s, 13-CH_3), 3.55 (3H, s, 7-CH_3), 3.72 (6H, s, 3-CH_3, 17-CH_3), 4.10 (3H, s, 18-CH_3), 4.12 (3H, s, $COOCH_3$), 5.97 (1H, m, 2^1-H), 7.56 (1H, ddd, J = 7, 7, 1 Hz, QH), 7.60 (1H, ddd, J = 7, 7, 1 Hz, QH), 7.66 (1H, d, J = 7 Hz, 2^4-H), 7.98 (1H, dd, J = 7, 1 Hz, QH), 8.10 (1H, dd, J = 7, 1 Hz, QH), 8.21 (1H, dd, J = 8, 1 Hz, 10Ar6-H), 8.29 (1H, dd, J = 8, 1 Hz, 10Ar2-H), 8.33 (1H, dd, J = 8, 1 Hz, 10Ar5-H, 8.36 (1H, dd, J = 8, 1 Hz, 10Ar3-H), 10.15 (1H, s, 5-H), 10.18 (1H, s, 15-H); MS m/z 778 (calcd for M^+, 778); UV/vis (CH_2Cl_2) 242, 269, 277, 408, 508, 584, 636 nm.

Instrumental Techniques. The ^{1}H NMR spectra were recorded on a Varian Unity spectrometer at 500 MHz. Unless otherwise specified, samples were dissolved in deuteriochloroform with tetramethylsilane as an internal reference. High-resolution mass spectra were obtained on a Kratos MS 50 mass spectrometer operating at 8 eV in FAB mode. Ultraviolet−visible spectra were measured on a Shimadzu UV2100U UV/vis spectrometer. Fluorescence spectra were measured on a SPEX Fluorolog using optically dilute samples and corrected. The solvent Raman signal was subtracted from the extremely low fluorescence emission from the dyad solutions. Cyclic voltammetric measurements were carried out with a Pine Instrument Co. Model AFRDE4 potentiostat. All electrochemical measurements were performed in benzonitrile at ambient temperatures with a glassy carbon working electrode, a Ag/Ag^+ reference electrode, and a platinum wire counter electrode. The electrolyte was 0.1 M tetra-*n*-butylammonium hexafluorophosphate, and ferrocene was employed as an internal reference redox system.

Fluorescence decay measurements were performed on $< 1 \times 10^{-5}$ M solutions by the time-correlated single photon counting method. All samples were purified either by column chromatography or by TLC prior to use. The excitation source was a frequency-doubled Coherent Antares 76s Nd:YAG laser routed through a variable beam splitter to pump a cavity dumped dye laser.[75] The instrument response function (35 ps) was measured at the excitation wavelength for each decay experiment with Ludox AS-40 under the same conditions as the sample.

Transient absorption measurements on the sub-picosecond time scale were made using the pump−probe technique. For ambient temperature measurements, the sample was dissolved in purified solvent and the resulting solution was circulated by magnetic stirring in a cuvette having a 2-mm path length in the beam area. Low-temperature measurements were performed using 2-mm path length cells mounted on the cold tip of a variable-temperature helium displex refrigerator (Air Products). The 25-mm diameter cell was constructed from quartz windows attached to a glass spacer ring with epoxy. Excitation was at 590 nm with 150−200 fs, 8-μJ pulses at a repetition rate of 540 Hz. The signals from the pump and continuum-generated white-light probe beam were collected by an optical spectrometric multichannel analyzer with a dual diode array detector head. Details are given elsewhere.[76]

Acknowledgment. This work was supported by a grant from the Division of Chemical Sciences, Office of Basic Energy Sciences, Office of Energy Research, U.S. Department of Energy (DE-FG03-93ER14404). We thank N. Woodbury for helpful discussions.

JA950098V

(74) Liddell, P. A.; Sumida, J. P.; Macpherson, A. N.; Noss, L.; Seely, G. R.; Clark, K. N.; Moore, A. L.; Moore, T. A.; Gust, D. *Photochem. Photobiol.* **1994**, *60*, 537−541.

(75) Gust, D.; Moore, T. A.; Luttrull, D. K.; Seely, G. R.; Bittersmann, E.; Bensasson, R. V.; Rougée, M.; Land, E. J.; de Schryver, F. C.; Van der Auweraer, M. *Photochem. Photobiol.* **1990**, *51*, 419−426.

(76) Lin, S.; Chiou, H.-C.; Kleinherenbrink, F. A. M.; Blankenship, R. E. *Biophys. J.* **1994**, *66*, 437−445.